MIKAILALSYS
Journal of Multidisciplinary Sciences

e-ISSN : 2987-2286
p-ISSN : 2987-3924
Index: Harvard, Boston, Sydney, Copernicus, Sinta 4, Scilit, Semantic, Google, etc

https://doi.org/10.58578/mikailalsys.v4i3.12344

Biosorption of Methylene Blue onto Fuji Appl Peel Biosorbent: Effects of Agitation Speeds and Contact Time

Putri Rahma Sari, Desy Kurniawati, Hary Sanjaya, Okta Suryani
Universitas Negeri Padang, Indonesia
desy.cem@gmail.com

Submitted:	Revised:	Accepted:	Published:
Sep 2, 2026	Oct 1, 2026	Oct 12, 2026	Oct 17, 2026

Abstract

Methylene blue (MB) is a cationic dye found in industrial wastewater that requires effective and environmentally sustainable treatment. This study investigated Fuji apple peel (*Malus domestica* 'Fuji') as a low-cost, renewable biosorbent for MB removal, focusing on contact time and agitation speed. Batch experiments used 0.2 g of biosorbent in 25 mL of MB solution at a constant initial concentration of 1100 mg/L. Contact times ranged from 30 to 150 min, and agitation speeds ranged from 100 to 300 rpm. Residual MB concentrations were measured using UV–Vis spectrophotometry at 665 nm, and adsorption capacities were calculated from concentration differences. Adsorption kinetics were evaluated using pseudo-first-order, pseudo-second-order, and intraparticle diffusion models. Adsorption capacity increased with contact time to 120.369 mg/g at 60 min, followed by a slight decline at longer durations. Increasing agitation speed enhanced MB uptake up to 250 rpm, yielding the highest observed capacity of 125.119 mg/g, whereas capacity decreased at 300 rpm. These findings identify 60 min and 250 rpm as the most favorable contact time and agitation speed within the investigated ranges. Fuji apple peel therefore shows potential as an inexpensive, renewable biosorbent for MB removal, supporting the use of fruit peel biomass in wastewater treatment development.

Keywords: Biosorption; Methylene Blue; Fuji Apple Peel; Contact Time; Agitation Speed

Mikailalsys is licensed under a Creative Commons Attribution-NonCommercial-ShareAlike 4.0 International License

INTRODUCTION

Synthetic dyes released from textile, printing, paper, leather, and other industrial activities are considered important aquatic pollutants because of their strong coloration and persistence in water (Guediri et al., 2019). Methylene blue (MB) is a cationic thiazine dye that is frequently used as a model pollutant in adsorption studies because of its intense color and chemical stability (Dinh et al., 2019). The presence of MB in aqueous environments can reduce water transparency and interfere with light penetration, making its removal an important environmental concern (Lin et al., 2022). Several treatment technologies have been investigated for dye-contaminated wastewater, including adsorption, membrane separation, coagulation, and advanced oxidation processes (Stavrinou et al., 2020). Among these technologies, adsorption has received considerable attention because of its relatively simple operation and effectiveness in removing dye molecules from aqueous solutions (Guediri et al., 2019).

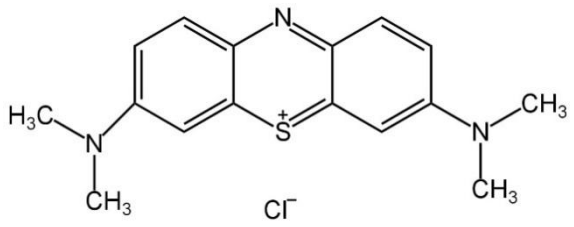


Figure 1. Chemical structure of *Methylene Blue* (MB)

The application of conventional activated carbon for dye removal can be limited by the cost associated with adsorbent production and regeneration (Maia et al., 2021). Therefore, agricultural residues and food-processing wastes have increasingly been investigated as alternative low-cost adsorbents for wastewater treatment (Stavrinou et al., 2020). Biomass-derived materials are attractive because they are abundant, renewable, and contain functional groups that can interact with contaminant molecules (Chen et al., 2021). Cellulose, hemicellulose, lignin, pectin, hydroxyl, and carboxyl groups present in plant-based materials can contribute to the binding of cationic dye molecules (Dinh et al., 2019). The utilization of agricultural residues as biosorbents can also provide an additional pathway for converting low-value biomass waste into useful materials for environmental applications (Maia et al., 2021).

Fruit peels are among the agricultural residues that have received considerable attention as biosorbents because of their lignocellulosic composition and surface functional

groups (Ren et al., 2018). Pomelo peel, for example, has demonstrated the ability to adsorb MB from aqueous solution through interactions between dye molecules and functional groups on the biosorbent surface (Dinh et al., 2019). The utilization of these residues as biosorbents can simultaneously support wastewater treatment and the valorization of agricultural waste (Chen et al., 2021). Therefore, fruit-processing residues represent attractive alternatives to conventional adsorbents for dye removal.

Apple-derived residues are particularly interesting because apple peel contains lignocellulosic components and oxygen-containing functional groups that can participate in adsorption interactions (Enniya & Jourani, 2017). Enniya & Jourani, (2017) demonstrated that apple peel could be used as a biosorbent for MB removal and evaluated its adsorption equilibrium, kinetics, and thermodynamic behavior (Enniya & Jourani, 2017). The adsorption of MB onto apple-processing residues has also been investigated using a solid residue generated by the apple juice industry, with equilibrium, thermodynamic, and kinetic characteristics being evaluated (Bonetto et al., 2021). These findings confirm the potential of apple-derived biomass for removing MB from aqueous solutions . More recently, apple-peel-derived activated carbon has been investigated as a precursor for the preparation of advanced adsorbents for MB removal, demonstrating continued interest in apple biomass for dye-treatment applications. However, the use of apple-derived materials in previous studies does not necessarily represent the adsorption behavior of every apple cultivar because biomass composition and surface characteristics can vary among plant varieties (Mohammadi et al., 2026)

Contact time is an important parameter because adsorption generally proceeds rapidly at the beginning and gradually approaches equilibrium as available adsorption sites become occupied (Enniya & Jourani, 2017). Kinetic models such as pseudo-first-order (PFO), pseudo-second-order (PSO), and intraparticle diffusion are commonly used to evaluate adsorption rates and possible rate-controlling mechanisms (Dinh et al., 2019). Comparison of these models provides more information about adsorption behavior than equilibrium capacity alone (Stavrinou et al., 2020). In addition, agitation speed influences mixing and mass transfer between MB molecules and biosorbent particles, thereby affecting adsorption performance (Wei et al., 2023).

Although apple peel has previously been investigated for MB removal, the apple cultivar used in the study of Enniya & Jourani, (2017) was not specifically identified. To the

best of our knowledge, the application of Fuji apple peel (*Malus domestica* 'Fuji') for MB biosorption, particularly in relation to contact-time kinetics and agitation speed, has not been specifically reported. This cultivar-specific investigation is important because differences in biomass characteristics may influence adsorption behavior (Bonetto et al., 2021). Therefore, this study investigates MB biosorption using Fuji apple peel by evaluating contact time and agitation speed.

The kinetic behavior of MB biosorption is evaluated using pseudo-first-order, pseudo-second-order, and intraparticle diffusion models to determine the adsorption rate and possible rate-controlling mechanism (Wei et al., 2023). The effect of agitation speed is also investigated to identify suitable mixing conditions for the biosorption process. This study is expected to provide new information on the potential of Fuji apple peel as a low-cost biosorbent for MB removal while contributing to the valorization of fruit-processing waste (Maia et al., 2021).

METHODS

1. Materials

Fuji apple peels (*Malus domestica* 'Fuji') were used as the biosorbent material for methylene blue (MB) removal. Methylene blue was used as the model cationic dye. Nitric acid (HNO_3) was used for chemical activation of the apple peel, while hydrochloric acid (HCl) and sodium hydroxide (NaOH) solutions were used to adjust the solution pH. Distilled water was used for solution preparation and washing of the biosorbent. All chemicals were of analytical grade and used without further purification.

2. Preparation and Activation of Biosorbent

Fresh Fuji apple peels were collected and separated from the remaining fruit material. The peels were initially washed thoroughly with tap water to remove adhering dirt and impurities and subsequently rinsed several times with distilled water. The cleaned peels were dried and then ground into a fine powder. The powder was sieved to obtain a uniform particle size of 125 μm.

Chemical activation was performed using 0.1 M HNO_3. The apple-peel powder was mixed with the HNO_3 solution and subjected to the activation process for 2 hours. After activation, the biosorbent was separated from the activating solution and washed repeatedly

with distilled water until the washing solution reached approximately neutral pH. The washed biosorbent was then dried in an oven at 60 °C until a constant mass was obtained. Constant mass was confirmed through three consecutive weighing measurements. The dried activated Fuji apple peel was subsequently stored in a dry and airtight container until use.

3. Biosorbent Characterization

Fourier transform infrared (FTIR) spectroscopy was used to identify the functional groups present in the activated Fuji apple peel before and after MB biosorption. The spectra were recorded in the range of 4000–400 cm^{-1}. Changes in the characteristic absorption bands, including shifts in peak position or changes in intensity after MB biosorption, were analyzed to identify functional groups potentially involved in the interaction between MB and the biosorbent surface.

4. Batch Biosorption Experiments

Batch experiments were conducted by mixing 0.2 g of HNO_3-activated Fuji apple peel with 25 mL of 1100 mg L^{-1} MB solution. The mixtures were agitated, filtered after treatment, and the residual MB concentration was measured at 665 nm using UV–Vis spectrophotometry. All experiments were performed in duplicate.

Contact-time experiments were conducted at 30, 60, 90, 120, and 150 min, while agitation speed was varied from 100 to 300 rpm (100, 150, 200, 250, and 300 rpm). The adsorption capacity was calculated as:

$$q_e = \frac{(C_0 - C_e)V}{m}$$

The kinetic data were analyzed using pseudo-first-order (PFO), pseudo-second-order (PSO), and intraparticle diffusion models. Model suitability was evaluated based on the regression coefficient (R^2) and the agreement between experimental and calculated adsorption capacities. The agitation speed giving the highest adsorption capacity was selected as the optimum condition.

RESULTS

1. FTIR Characterization of Biosorbent.

The Fourier transform infrared (FTIR) spectra of the Fuji apple peel biosorbent before activation (FAP), after nitric acid activation (FAP-A), and after contact with Methylene Blue (FAP-A/MB) are presented in Figure 1. The FTIR analysis was performed to identify the main functional groups present on the biosorbent surface and to observe changes in the characteristic absorption bands following activation and MB biosorption.

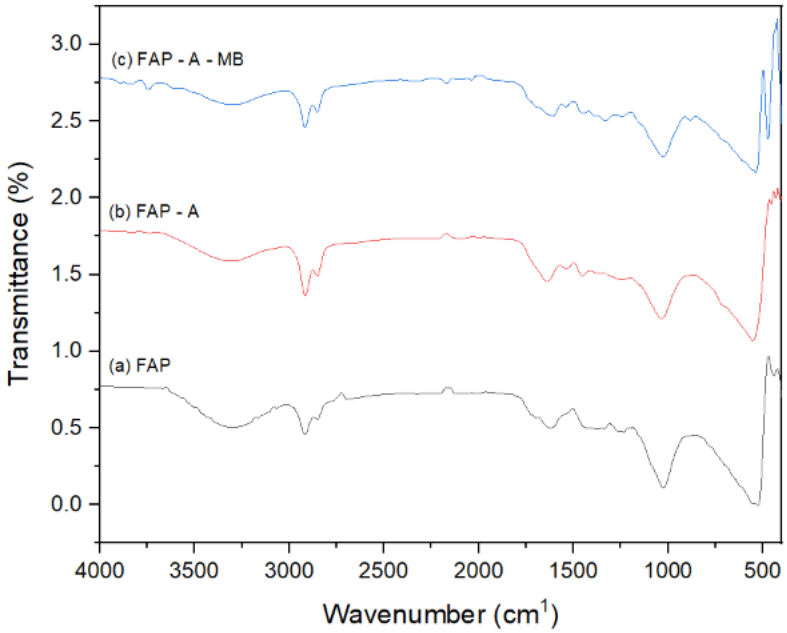


Figure 2. FTIR Spektrum of (a) Fuji apple pell (FAP), (b) Fuji apple peel-activated (FAP-A), (c) Fuji apple peel activated after contact with *methylene blue* (FAP-A-MB)

The FTIR spectrum of FAP exhibited several characteristic absorption bands associated with the organic components of the apple peel. A broad absorption band was observed around 3297.70 cm^{-1}, which was attributed to O–H stretching vibrations. The bands at 2917.66 and 2854.48 cm^{-1} corresponded to C–H stretching vibrations of aliphatic groups. Additional absorption bands were observed in the fingerprint region, particularly within the ranges associated with C–O and other oxygen-containing functional groups.

After nitric acid activation, changes in the intensity and position of several absorption bands were observed in the FAP-A spectrum. The broad O–H band was observed at approximately 3362 cm^{-1}, while the characteristic aliphatic C–H stretching region remained evident. Absorption bands in the 1300–900 cm^{-1} region were also observed, corresponding mainly to C–O-containing functional groups. These spectral features indicate that the major

functional groups characteristic of the Fuji apple peel biosorbent remained present following the activation treatment.

Following contact with MB, the FTIR spectrum of FAP-A/MB showed changes in several characteristic absorption bands compared with the FAP-A spectrum. The O–H stretching band was observed at approximately 3342 cm^{-1}, while changes were also observed in the bands associated with aliphatic C–H and C–O-containing groups. The spectral changes observed after MB contact indicate differences in the infrared response of the biosorbent surface following interaction with MB.

2. Effect of Contact Time

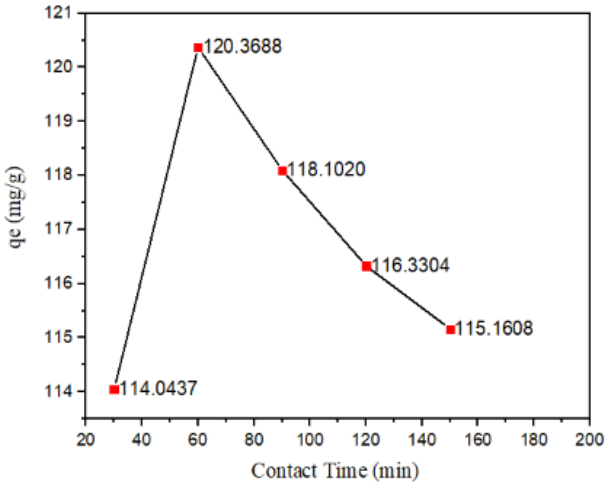


Figure 3. Effect contact time of FAP-A on MB Dye Biosorption

The effect of contact time on the biosorption capacity of Methylene Blue (MB) onto Fuji apple peel biosorbent is presented in Figure 1. The biosorption capacity increased from 114.044 mg/g at 30 min to 120.369 mg/g at 60 min. After reaching the maximum value at 60 min, the biosorption capacity decreased to 118.052 mg/g at 90 min, 116.385 mg/g at 120 min, and 115.048 mg/g at 150 min. Among the investigated contact times, 60 min resulted in the highest biosorption capacity of 120.369 mg/g. Therefore, a contact time of 60 min was selected as the optimum condition for the subsequent experiments.

3. Effect of agitation speed

The influence of agitation speed on the biosorption capacity of MB is shown in Figure 2. The biosorption capacity increased progressively from 111.5029 mg/g at 100 rpm

to 115.2109 mg/g at 150 rpm and 120.6542 mg/g at 200 rpm. The maximum biosorption capacity of 125.1193 mg/g was obtained at 250 rpm. However, a further increase in agitation speed resulted in a decrease in biosorption capacity, with values of 118.3370 mg/g at 300 rpm and 110.3810 mg/g at 350 rpm. Thus, 250 rpm was identified as the optimum agitation speed, providing the highest biosorption capacity among the investigated conditions.

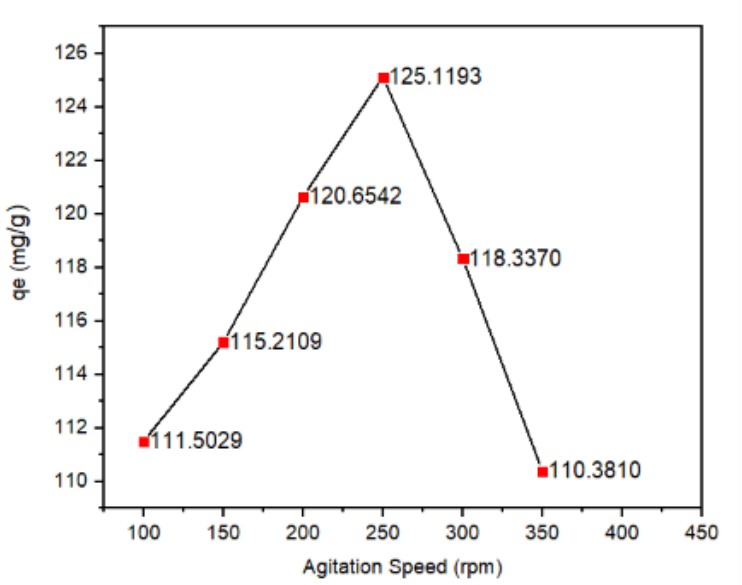


Figure 3. Effect agitation speed of FAP-A on MB Dye Biosorption

4. Kinetics Modeling

The adsorption kinetics of MB onto Fuji apple peel biosorbent were evaluated using the pseudo-first-order (PFO), pseudo-second-order (PSO), and intraparticle diffusion models. The corresponding kinetic plots are presented in Figure 3. The regression equations and correlation coefficients obtained from each kinetic model are summarized in Table 1.

The kinetic parameters obtained from the PFO and PSO models were compared with the experimental biosorption capacity. The model exhibiting the highest coefficient of determination (R^2) was considered to provide the best fit to the experimental kinetic data. The intraparticle diffusion model was additionally used to evaluate the contribution of diffusion processes to the biosorption of MB onto the Fuji apple peel biosorbent.

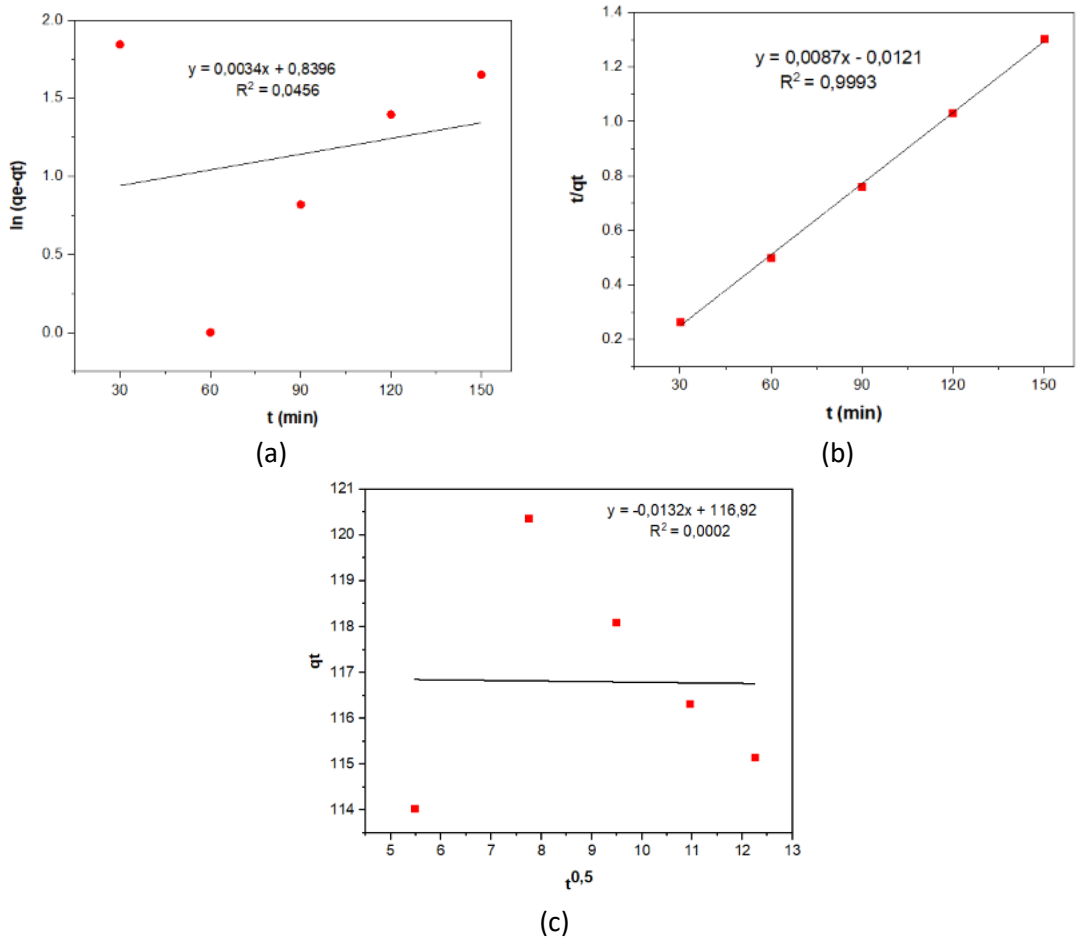


Figure 4. Kinetic plots of Methylene Blue biosorption onto Fuji apple peel biosorbent using (a) pseudo-first-order, (b) pseudo-second-order, and (c) intraparticle diffusion models

Table 1. Kinetic parameters for Methylene Blue biosorption onto Fuji apple peel biosorbent

Kinetic Model	Parameter	Result
Pseudo-first-order	$q_{e,exp}$ (mg. g^{-1})	120.369
	k_1(min^{-1})	0.0015
	$q_{e,cal}$(mg. g^{-1})	4.8673
	R^2	0.0456
Pseudo-second-order	k_2 (g. mg^{-1}. min^{-1})	0.006
	$q_{e,cal}$ (mg g^{-1})	114.7628
	R^2	0.9993
Intraparticle diffusion	k_{diff}(mg. g^{-1}. min$^{-1/2}$)	0.0225
	C (mg. g^{-1})	116.9862
	R^2	0.0002

DISCUSSION

1. FTIR Characterization of Biosorbent.

FTIR analysis was performed to identify the functional groups present in Fuji apple peel before and after HNO_3 activation and to evaluate changes in the biosorbent surface after methylene blue (MB) adsorption. The FTIR spectra of untreated Fuji apple peel (FAP), HNO_3-activated Fuji apple peel (FAP-A), and FAP-A after contact with MB are presented in Figure 2. The spectra showed characteristic absorption bands associated with hydroxyl, aliphatic C–H, carbonyl/aromatic, and C–O-containing groups, which are commonly found in lignocellulosic biosorbents (Stavrinou et al., 2020).

The untreated Fuji apple peel exhibited a broad absorption band at 3297.90 cm^{-1}, which can be assigned to O–H stretching vibrations of hydroxyl groups present in the lignocellulosic structure (Mahadlek & Mahadlek, 2020). The bands at 2917.66 and 2854.48 cm^{-1} are associated with C–H stretching vibrations of aliphatic groups commonly present in plant-based adsorbents (Stavrinou et al., 2020). The absorption band at 1619.44 cm^{-1} can be related to C=O and/or aromatic skeletal vibrations, whereas the bands at 1242.44 and 1024.98 cm^{-1} are associated with C–O-containing structures in lignocellulosic materials (Sharma et al., 2022). The presence of these oxygen-containing functional groups indicates that untreated Fuji apple peel possesses potential active sites for interaction with dye molecules .

After HNO_3 activation, the O–H band shifted from 3297.90 to 3292.71 cm^{-1}, indicating a change in the chemical environment of hydroxyl groups following acid treatment (Gupta et al., 2022). The C–H bands also shifted slightly from 2917.66 and 2854.48 cm^{-1} to 2916.15 and 2852.01 cm^{-1}, respectively, suggesting changes in the surrounding chemical environment of aliphatic groups after activation (Ahmad et al., 2021). The band near 1619.44 cm^{-1} shifted to 1637.25 cm^{-1}, while additional bands appeared at 1536.66 and 1452.95 cm^{-1}, indicating changes in the surface structure following HNO_3 treatment (Gupta et al., 2022). Similar modifications of FTIR bands after chemical treatment have been reported for fruit-derived activated adsorbents.

The bands in the fingerprint region also exhibited changes after activation. The band at 1242.44 cm^{-1} shifted slightly to 1243.11 cm^{-1}, while the band at 1024.98 cm^{-1} shifted to 1034.53 cm^{-1}, indicating changes involving C–O-containing functional groups (Sharma et

al., 2022). Similar C–O-related absorption bands have been reported in fruit-peel-based adsorbents and are generally associated with cellulose, hemicellulose, and lignin structures (Stavrinou et al., 2020). These changes suggest that HNO_3 treatment modified the surface chemical environment of the Fuji apple peel while retaining its major lignocellulosic functional groups (Gupta et al., 2022).

After contact with MB, several characteristic bands of the activated biosorbent changed in position. The O–H band shifted from 3292.71 to 3280.79 cm^{-1}, suggesting that hydroxyl-containing groups may have participated in interactions with MB molecules (Mahadlek & Mahadlek, 2020). The C–H stretching bands changed from 2916.15 and 2852.01 cm^{-1} to 2916.99 and 2851.66 cm^{-1}, respectively, indicating changes in the chemical environment of aliphatic groups after MB uptake (Stavrinou et al., 2020). Similar changes in FTIR bands after MB adsorption have been reported for banana-peel and other biomass-based adsorbents (Ezetty & Alias, 2018).

A notable change occurred around the 1600 cm^{-1} region, where the band shifted from 1637.25 cm^{-1} before adsorption to 1606.74 cm^{-1} after MB contact. Changes in this region can be associated with carbonyl and aromatic structures that may participate in interactions with adsorbed MB molecules (Sharma et al., 2022). Similar changes in FTIR bands around 1600–1650 cm^{-1} have been observed after MB adsorption onto fruit-derived biosorbents (Dinh et al., 2019). However, because FTIR peak shifts alone cannot establish a single adsorption mechanism, the observed change should be interpreted as evidence of an altered chemical environment rather than definitive proof of a specific interaction (Mahadlek & Mahadlek, 2020).

Changes were also observed in the fingerprint region after MB contact. The band at 1243.11 cm^{-1} shifted to 1245.19 cm^{-1}, while the band at 1034.53 cm^{-1} shifted to 1025.42 cm^{-1}, suggesting changes involving C–O-containing groups following MB adsorption (Ahmad et al., 2021). The appearance of bands at 1332.43 and 883.70 cm^{-1} after MB contact further indicates changes in the fingerprint region of the biosorbent. Similar changes in C–O-containing regions have been reported following dye adsorption onto lignocellulosic biomass (Stavrinou et al., 2020).

Overall, the FTIR spectra demonstrate that HNO_3 activation altered the chemical environment of the Fuji apple peel surface, while subsequent MB contact produced

additional changes in several characteristic absorption bands (Gupta et al., 2022). The shifts observed in the O–H, C–H, approximately 1600 cm^{-1}, and C–O regions suggest the involvement of oxygen-containing and other surface functional groups in MB biosorption (Ezetty & Alias, 2018). Previous FTIR studies of fruit-peel biosorbents have similarly associated changes in these functional-group regions with interactions between cationic MB and biosorbent surfaces (Dinh et al., 2019). Therefore, the FTIR results support the participation of surface functional groups in the biosorption of MB by HNO_3-activated Fuji apple peel.

2. Effect of Contact Time

Contact time is an important parameter in biosorption because it determines the duration of interaction between methylene blue (MB) molecules and the active sites of the Fuji apple peel (FAP) biosorbent. As shown in Figure 3, the adsorption capacity increased from 114.0437 mg g^{-1} at 30 min to a maximum of 120.3688 mg g^{-1} at 60 min, followed by a gradual decrease to 115.1608 mg g^{-1} at 150 min, indicating that extending the contact time initially enhanced MB uptake. The rapid increase during the initial stage can be attributed to the abundance of vacant and readily accessible adsorption sites on the biosorbent surface, which facilitates the transfer of MB molecules from the solution to the biosorbent surface (Ma et al., 2018). The relatively rapid uptake also indicates that the active sites involved in MB binding were sufficiently accessible during the early adsorption period. Similar initial adsorption behavior has been reported for fruit-peel-based biosorbents, where rapid dye uptake occurred during the early stage because of the availability of accessible surface sites (Farias et al., 2023).

The high adsorption capacity obtained within the first 60 min can also be explained by the concentration gradient between MB molecules in the aqueous solution and the FAP surface. A higher concentration gradient provides a greater driving force for mass transfer, promoting the movement of MB molecules toward available binding sites on the biosorbent (Singh et al., 2020). As contact time increased, the number of readily accessible sites progressively decreased, while the concentration gradient became less pronounced, resulting in a lower net adsorption rate (Holliday et al., 2024). Consequently, the system reached its highest measured adsorption capacity at 60 min. The subsequent decrease in adsorption capacity from 120.3688 mg g^{-1} at 60 min to 115.1608 mg g^{-1} at 150 min suggests that prolonged contact did not provide additional net MB uptake under the investigated

conditions. Although site occupation can contribute to the reduction in adsorption rate, the decrease in measured capacity after 60 min should not be attributed exclusively to site saturation because other processes, such as adsorption–desorption re-equilibration or experimental variation, may also contribute.

The contact-time behavior observed in this study is generally consistent with previous reports on fruit-derived biosorbents. Ates & Oymak (2020) reported that adsorption using biomass-based materials commonly proceeds rapidly at the beginning and gradually approaches equilibrium as the available adsorption sites become increasingly occupied. Similarly, Lin et al. (2022) reported effective MB adsorption by fruit-peel-based biosorbents within a relatively short contact period, demonstrating that lignocellulosic biomass can provide accessible functional groups for interaction with cationic dyes. The maximum adsorption capacity of FAP at 60 min in the present study therefore indicates a comparable rapid adsorption tendency. However, direct comparison of optimum contact times among different studies should be made cautiously because adsorption behavior is strongly affected by biosorbent characteristics, initial dye concentration, adsorbent dosage, particle size, pH, agitation speed, and solution volume (Ates & Oymak, 2020).

From a practical perspective, the attainment of the maximum adsorption capacity within 60 min is an important finding because it indicates that extending the treatment period to 90–150 min did not improve MB uptake under the experimental conditions used in this study. Therefore, 60 min can be considered an appropriate operating time for the FAP biosorbent, providing a relatively high adsorption capacity while avoiding unnecessary extension of the treatment period. This finding is particularly relevant for the potential application of FAP as a low-cost biosorbent because shorter treatment times can improve process efficiency and reduce the time required for batch adsorption operations. The result also supports the potential utilization of Fuji apple peel waste as an alternative biomass material for MB removal from aqueous systems.

Nevertheless, the optimum contact time of 60 min should be interpreted within the limitations of the present experimental conditions. The observed adsorption behavior was obtained at the selected MB concentration, biosorbent dosage, particle size, pH, agitation speed, and solution volume; therefore, the optimum time may change when these parameters are altered. In addition, the gradual decrease in adsorption capacity after 60 min was determined from the measured experimental values and was not independently confirmed

by desorption or equilibrium studies. Further investigation using replicated experiments, equilibrium analysis, and desorption studies would be useful to clarify the mechanism responsible for the post-60-min decrease and to determine whether the observed maximum represents true adsorption equilibrium. Based on the experimental results, however, 60 min was selected as the optimum contact time because it produced the highest measured adsorption capacity of 120.3688 mg g^{-1}.

3. Effect of agitation speed

Agitation speed is an important operating parameter in biosorption because it affects the mixing intensity, particle dispersion, and mass transfer between methylene blue (MB) molecules and the Fuji apple peel (FAP) biosorbent. As shown in Figure 4, the adsorption capacity increased from 111.5029 mg g^{-1} at 100 rpm to 115.2109 mg g^{-1} at 150 rpm, 120.6542 mg g^{-1} at 200 rpm, and reached a maximum of 125.1193 mg g^{-1} at 250 rpm. The increase in adsorption capacity with agitation speed indicates that stronger mixing enhanced the contact between MB molecules and the available adsorption sites on FAP. Increasing agitation can reduce the thickness of the liquid boundary layer surrounding biosorbent particles and consequently facilitate the transfer of dye molecules from the bulk solution toward the biosorbent surface (Dotto & Pinto, 2012). Similar enhancement of MB uptake with increasing agitation has been reported for algal biomass, where higher agitation improved dye distribution and reduced particle aggregation, resulting in more effective interaction between the dye and biosorbent (Maurya et al., 2014).

The gradual increase in adsorption capacity from 111.5029 to 125.1193 mg g^{-1} between 100 and 250 rpm represents an increase of approximately 12.21%. This behavior suggests that agitation at 100 rpm was not sufficient to maximize the mass transfer of MB to the FAP surface, whereas agitation at 250 rpm provided more effective dispersion of the biosorbent particles in the solution. Greater mixing increases the frequency of collisions between MB molecules and biosorbent particles and can improve the accessibility of adsorption sites (Hameed, 2009). The importance of agitation in promoting mass transfer has also been demonstrated for methylene blue biosorption using agricultural waste, where an intermediate agitation speed produced the most favorable adsorption performance because the biosorbent particles were adequately dispersed in the dye solution (Holliday et al., 2024).

The maximum adsorption capacity of 125.1193 mg g^{-1} at 250 rpm indicates that this agitation speed provided the most favorable hydrodynamic condition for MB biosorption onto FAP. However, increasing the agitation speed beyond this optimum resulted in a decrease in adsorption capacity to 118.3370 mg g^{-1} at 300 rpm and 110.3810 mg g^{-1} at 350 rpm. The decrease from 250 to 350 rpm corresponds to approximately 11.78%, demonstrating that excessive agitation was not beneficial for MB uptake under the experimental conditions. A similar optimum-type behavior has been reported for agricultural pea waste, where an intermediate agitation speed produced the most favorable MB adsorption, whereas higher agitation resulted in reduced adsorption, possibly because excessive mixing altered the dispersion of the biosorbent particles (Holliday et al., 2024). Therefore, the present results indicate that increasing agitation speed does not necessarily produce a continuously increasing adsorption capacity.

The decrease observed at 300–350 rpm can be associated with changes in the hydrodynamic conditions of the biosorption system. Once the external mass-transfer resistance has been sufficiently reduced, further increases in agitation may provide limited improvement in MB transport to the biosorbent surface (Maurya et al., 2014). Excessive agitation may also increase particle–particle collisions and disturb weakly bound MB molecules on the biosorbent surface, potentially contributing to partial desorption and the observed decline in adsorption capacity (Holliday et al., 2024). Similar observations have been reported in recent MB adsorption studies, where adsorption performance increased with agitation until an optimum speed and subsequently decreased at higher speeds because of excessive turbulence and possible detachment of previously adsorbed dye molecules .

The optimum agitation speed of 250 rpm obtained in this study is comparable with the range reported for other biomass-based MB adsorption systems, although the optimum value varies according to the properties of the biosorbent and experimental conditions. Adaramola et al., (2024) reported an optimum agitation speed of 150 rpm for MB adsorption onto *Roystonea regia* fruit pericarp, with an adsorption capacity of 132.30 mg g^{-1} (Adaramola et al., 2024). Agricultural pea waste has also been reported to exhibit its most favorable MB adsorption performance at an intermediate agitation speed, demonstrating that excessive agitation does not necessarily enhance adsorption capacity (Holliday et al., 2024). Differences between the optimum speeds reported in the literature and the present study can be attributed to differences in biosorbent structure, particle size, adsorbent dosage, initial dye

concentration, pH, and other operating conditions . Thus, the optimum agitation speed of 250 rpm obtained in this study should be considered specific to the FAP–MB system under the experimental conditions investigated.

Based on these results, 250 rpm was selected as the optimum agitation speed, as it produced the highest experimental adsorption capacity of 125.1193 mg g^{-1}. Nevertheless, a limitation of this analysis is that the specific mechanism responsible for the decrease above 250 rpm cannot be confirmed solely from adsorption-capacity data (Shelke et al., 2022). Additional analyses, such as desorption experiments, particle-size evaluation, or surface characterization after agitation, would be required to determine whether excessive agitation causes changes in particle structure or partial release of weakly bound MB molecules (Holliday et al., 2024). Therefore, 250 rpm was selected as the optimum agitation speed for subsequent experiments, as it produced the highest adsorption capacity among all tested conditions.

4. Kinetics Modeling

The adsorption kinetics of Methylene Blue (MB) onto Fuji apple peel biosorbent were evaluated using pseudo-first-order (PFO), pseudo-second-order (PSO), and intraparticle diffusion models to determine the kinetic behavior and possible rate-controlling processes. These models are commonly used to describe adsorption rates and to evaluate the contribution of surface adsorption and diffusion during the uptake of dye molecules by biomass-based adsorbents. Recent studies have applied these kinetic models to MB adsorption using fruit peels and other agricultural-derived materials, demonstrating that the suitability of each model depends strongly on the characteristics of the adsorbent and experimental conditions (Ton-that et al., 2023).

The pseudo-first-order model describes adsorption in which the adsorption rate is related to the number of available adsorption sites and the difference between the adsorption capacity at equilibrium and at a specific contact time. In the present study, the PFO model showed a lower agreement with the experimental data than the PSO model, indicating that this model was not sufficient to describe the overall MB uptake by Fuji apple peel. Similar results have been reported for MB adsorption onto pomelo fruit peel, where the PFO model showed a lower correlation than the PSO and other kinetic models (Dinh et al., 2019). A study using jackfruit-peel-derived biochar also reported that the PFO model provided a weaker fit compared with the PSO and Elovich models, suggesting that the adsorption rate

could not be adequately explained by the PFO assumption alone (Ton-that et al., 2023). Therefore, the lower fitting performance of the PFO model in the present study suggests that MB biosorption onto Fuji apple peel involves adsorption processes that are more complex than a single first-order rate behavior.

The pseudo-second-order model provided the best fit to the experimental kinetic data, as indicated by the highest coefficient of determination among the models evaluated. The regression analysis gave an (R^2) value of approximately 0.9993, demonstrating an excellent agreement between the experimental adsorption capacity and the value predicted by the PSO model. The calculated equilibrium adsorption capacity was approximately 114.86 mg/g, which was relatively close to the experimental adsorption capacity obtained in the contact-time experiment. Similar behavior has been reported for MB adsorption using pomegranate peel, where the PSO model provided a better description of the adsorption kinetics than the PFO model (Ghibate et al., 2024). A recent study using activated carbon derived from jackfruit peel also reported an excellent PSO fit for MB adsorption, with an (R^2) value of 1.000 under the optimum experimental conditions (Aziz et al., 2026). These results indicate that the PSO model can effectively describe the overall rate of MB uptake by fruit-derived biosorbents, although the model fit alone should not be interpreted as definitive evidence of a specific molecular adsorption mechanism.

The intraparticle diffusion model was applied to determine whether diffusion of MB molecules into the internal pores of Fuji apple peel was the main rate-controlling step. The model showed a very weak correlation with the experimental data compared with the PSO model, indicating that intraparticle diffusion alone could not adequately describe the adsorption process. In addition, the regression line did not pass through the origin, suggesting that other processes contributed to the overall adsorption rate. Similar behavior was observed for MB adsorption onto pomelo fruit peel, where the intraparticle diffusion model did not pass through the origin, indicating that adsorption involved multiple stages rather than being controlled solely by diffusion within the particles (Dinh et al., 2019). Ton-That et al., (2023) also found that intraparticle diffusion was not the dominant kinetic model for MB adsorption onto jackfruit-peel-derived biochar. Thus, MB biosorption onto Fuji apple peel likely involves an initial transfer of MB molecules from the bulk solution to the external biosorbent surface, followed by interaction with available surface sites and subsequent diffusion into the particle structure.

The kinetic behavior was consistent with the experimental contact-time profile, in which the adsorption capacity increased rapidly from 114.0437 mg/g at 30 min to 120.3688 mg/g at 60 min, followed by a gradual decrease to 118.1020, 116.3304, and 115.1608 mg/g at 90, 120, and 150 min, respectively. The rapid adsorption during the first 60 min can be attributed to the high availability of accessible adsorption sites and the strong concentration gradient between MB molecules in solution and the biosorbent surface. Rapid initial uptake followed by a slower adsorption stage has also been reported for fruit-peel-based adsorbents, including pomelo peel and pomegranate peel, where the initially available active sites facilitate rapid dye uptake before becoming progressively occupied (Ghibate et al., 2024). The decrease in adsorption capacity after 60 min may indicate that most readily accessible adsorption sites had already been occupied, while adsorption and desorption processes approached a dynamic equilibrium.

Overall, the kinetic analysis demonstrates that the pseudo-second-order model was the most appropriate model for describing MB biosorption onto Fuji apple peel, while the intraparticle diffusion model indicated that diffusion within the biosorbent particles was not the sole rate-controlling process. The dominance of the PSO model is consistent with several recent studies of MB adsorption using fruit-derived adsorbents, although the dominant kinetic model can vary depending on the structure and surface properties of the biosorbent (Ton-That et al., 2023). The maximum experimental adsorption capacity obtained at 60 min, namely 120.3688 mg/g, therefore indicates that 60 min represents the most effective contact time under the present experimental conditions. This result further demonstrates that Fuji apple peel has considerable potential as a low-cost biosorbent for MB removal from aqueous solution.

CONCLUSION

Fuji apple peel demonstrated considerable potential as a low-cost and biomass-based biosorbent for Methylene Blue removal from aqueous solution. The biosorption process was influenced by both contact time and agitation speed, with the highest biosorption capacity obtained at a contact time of 60 min (120.369 mg/g) and an agitation speed of 250 rpm (125.1193 mg/g). FTIR characterization confirmed the presence of O–H, C–H, and C–O functional groups on the Fuji apple peel surface and revealed changes in the characteristic absorption bands following MB biosorption. Kinetic analysis indicated that the pseudo-

second-order model provided the best fit to the experimental data, with a high coefficient of determination (R^2 = 0.99924), suggesting that this model most appropriately described the biosorption kinetics under the investigated conditions. The findings contribute to the field of biosorption by demonstrating the potential utilization of Fuji apple peel, an agricultural biomass residue, as an alternative biosorbent for Methylene Blue removal and by establishing suitable operating conditions for the biosorption process. Future studies should investigate the underlying biosorption mechanism through additional surface characterization, evaluate the regeneration and reusability of the biosorbent, and assess its performance using real textile wastewater and continuous-flow adsorption systems to determine its practical applicability.

REFERENCES

Adaramola, F. B., Babarinde, N. A. A., Osobamiro, T. M., & Ibikunle, A. A. (2024). Adsorptive sequestration of methylene blue dye from aqueous solution using novel *Roystonea regia* fruit pericarp: Isotherm, kinetics, and thermodynamics. *Gazi University Journal of Science, 37*(2), 813–838. https://doi.org/10.35378/gujs.1218734

Ahmad, M. A., Eusoff, M. A., Oladoye, P. O., Adegoke, K. A., & Bello, O. S. (2021). Optimization and batch studies on adsorption of methylene blue dye using pomegranate fruit peel based adsorbent. *Chemical Data Collections, 32*, Article 100676. https://doi.org/10.1016/j.cdc.2021.100676

Ates, A., & Oymak, T. (2020). Characterization of persimmon fruit peel and its biochar for removal of methylene blue from aqueous solutions: Thermodynamic, kinetic and isotherm studies. *International Journal of Phytoremediation, 22*(6), 607–616. https://doi.org/10.1080/15226514.2019.1696745

Aziz, R. A., Tahiruddin, N. S. M., Ali, R., & Taib, N. I. (2026). Fruit waste to wealth: Adsorption isotherm, kinetics, and thermodynamic studies of methylene blue removal using activated carbon derived from jackfruit peel (*Artocarpus heterophyllus*). *Next Materials, 11*, Article 101901. https://doi.org/10.1016/j.nxmate.2026.101901

Bonetto, L. R., Crespo, J. S., Guégan, R., Esteves, V. I., & Giovanela, M. (2021). Removal of methylene blue from aqueous solutions using a solid residue of the apple juice industry: Full factorial design, equilibrium, thermodynamics and kinetics aspects. *Journal of Molecular Structure, 1224*, Article 129296. https://doi.org/10.1016/j.molstruc.2020.129296

Chen, K., Du, L., Gao, P., Zheng, J., Liu, Y., & Lin, H. (2021). Super and selective adsorption of cationic dyes onto carboxylate-modified passion fruit peel biosorbent. *Frontiers in Chemistry, 9*, Article 646492. https://doi.org/10.3389/fchem.2021.646492

Dinh, V.-P., Huynh, T.-D.-T., Le, H. M., Nguyen, V.-D., Dao, V.-A., Hung, N. Q., Tuyen, L. A., Lee, S., Yi, J., Nguyen, T. D., & Tan, L. V. (2019). Insight into the adsorption mechanisms of methylene blue and chromium(III) from aqueous solution onto pomelo fruit peel. *RSC Advances, 9*(44), 25847–25860. https://doi.org/10.1039/c9ra04296b

Dotto, G. L., & Pinto, L. A. A. (2012). Analysis of mass transfer kinetics in the biosorption of synthetic dyes onto *Spirulina platensis* nanoparticles. *Biochemical Engineering Journal, 68*, 85–90. https://doi.org/10.1016/j.bej.2012.07.010

Enniya, I., & Jourani, A. (2017). Study of methylene blue removal by a biosorbent prepared with apple peels. *Journal of Materials and Environmental Sciences, 8*(12), 4573–4581. https://doi.org/10.26872/jmes.2017.8.12.883

Farias, K. C. S., Guimarães, R. C. A., Oliveira, K. R. W., Nazário, C. E. D., Ferencz, J. A. P., & Wender, H. (2023). Banana peel powder biosorbent for removal of hazardous organic pollutants from wastewater. *Toxics, 11*(8), Article 664. https://doi.org/10.3390/toxics11080664

Ghibate, R., Ben Baaziz, M., Amechrouq, A., Taouil, R., & Senhaji, O. (2024). The performance of an eco-friendly adsorbent for methylene blue removal from aqueous solution: Kinetic, isotherm and thermodynamic approaches. *Journal of the Serbian Chemical Society, 89*(7–8), 1107–1121. https://doi.org/10.2298/JSC230317037G

Guediri, A., Bouguettoucha, A., Chebli, D., Chafai, N., & Amrane, A. (2020). Molecular dynamic simulation and DFT computational studies on the adsorption performances of methylene blue in aqueous solutions by orange peel-modified phosphoric acid. *Journal of Molecular Structure, 1202*, Article 127290. https://doi.org/10.1016/j.molstruc.2019.127290

Gupta, S. A., Vishesh, Y., Sarvshrestha, N., Bhardwaj, A. S., Kumar, P. A., Topare, N. S., Raut-Jadhav, S., Bokil, S. A., & Khan, A. (2022). Adsorption isotherm studies of methylene blue using activated carbon of waste fruit peel as an adsorbent. *Materials Today: Proceedings, 57*, 1500–1508. https://doi.org/10.1016/j.matpr.2021.12.044

Hameed, B. H. (2009). Removal of cationic dye from aqueous solution using jackfruit peel as non-conventional low-cost adsorbent. *Journal of Hazardous Materials, 162*(1), 344–350. https://doi.org/10.1016/j.jhazmat.2008.05.045

Holliday, M. C., Parsons, D. R., & Zein, S. H. (2024). Agricultural pea waste as a low-cost pollutant biosorbent for methylene blue removal: Adsorption kinetics, isotherm and thermodynamic studies. *Biomass Conversion and Biorefinery, 14*(5), 6671–6685. https://doi.org/10.1007/s13399-022-02865-8

Lin, H., Chen, K., Du, L., Gao, P., Zheng, J., Liu, Y., & Ma, L. (2022). Efficient and selective adsorption of methylene blue and methyl violet dyes by yellow passion fruit peel. *Environmental Technology, 43*(23), 3519–3530. https://doi.org/10.1080/09593330.2021.1924288

Ma, L., Jiang, C., Lin, Z., & Zou, Z. (2018). Microwave-hydrothermal treated grape peel as an efficient biosorbent for methylene blue removal. *International Journal of Environmental Research and Public Health, 15*(2), Article 239. https://doi.org/10.3390/ijerph15020239

Mahadlek, J., & Mahadlek, J. (2020). Investigation of various factors affecting methylene blue adsorption on agricultural waste: Banana stalks. *Science, Engineering and Health Studies, 14*(1), 47–61. https://doi.org/10.14456/sehs.2020.5

Maia, L. S., Duizit, L. D., Pinhatio, F. R., & Mulinari, D. R. (2021). Valuation of banana peel waste for producing activated carbon via NaOH and pyrolysis for methylene blue removal. *Carbon Letters, 31*(4), 749–762. https://doi.org/10.1007/s42823-021-00226-5

Maurya, R., Ghosh, T., Paliwal, C., Shrivastav, A., Chokshi, K., Pancha, I., Ghosh, A., & Mishra, S. (2014). Biosorption of methylene blue by de-oiled algal biomass: Equilibrium, kinetics and artificial neural network modelling. *PLoS ONE, 9*(10), Article e109545. https://doi.org/10.1371/journal.pone.0109545

Mohammadi, P., Khajenoori, M., & Ghandali, M. (2026). Synthesis of magnetite nanocomposite supported on apple peel-derived activated carbon for removal of methylene blue from aqueous solutions. *Scientific Reports, 16*(1), Article 14617. https://doi.org/10.1038/s41598-026-42265-w

Ren, Y., Cui, C., & Wang, P. (2018). Pomelo peel modified with citrate as a sustainable adsorbent for removal of methylene blue from aqueous solution. *Molecules, 23*(6), Article 1342. https://doi.org/10.3390/molecules23061342

Sharma, S., Sharma, G., Kumar, A., AlGarni, T. S., Naushad, M., ALOthman, Z. A., & Stadler, F. J. (2022). Adsorption of cationic dyes onto carrageenan and itaconic acid-based superabsorbent hydrogel: Synthesis, characterization and isotherm analysis. *Journal of Hazardous Materials, 421*, Article 126729. https://doi.org/10.1016/j.jhazmat.2021.126729

Singh, R., Singh, T. S., Odiyo, J. O., Smith, J. A., & Edokpayi, J. N. (2020). Evaluation of methylene blue sorption onto low-cost biosorbents: Equilibrium, kinetics, and thermodynamics. *Journal of Chemistry, 2020*, Article 8318049. https://doi.org/10.1155/2020/8318049

Stavrinou, A., Aggelopoulos, C. A., & Tsakiroglou, C. D. (2020). A methodology to estimate the sorption parameters from batch and column tests: The case study of methylene blue sorption onto banana peels. *Processes, 8*(11), Article 1467. https://doi.org/10.3390/pr8111467

Ton-That, L., Huynh, T.-N.-L., Duong, B.-N., Nguyen, D.-K., Nguyen, N.-A., Pham, V.-H., Ho, T.-H., & Dinh, V.-P. (2023). Kinetic studies of the removal of methylene blue from aqueous solution by biochar derived from jackfruit peel. *Environmental Monitoring and Assessment, 195*(11), Article 1266. https://doi.org/10.1007/s10661-023-11867-6

Ton-That, L., Pham, H.-D., Huynh, T.-N.-L., Duong, B.-N., Luu, T.-T., Nguyen, D.-K., Nguyen, N.-A., Ho, T.-H., Pham, V.-H., & Dinh, V.-P. (2023). Adsorption of methylene blue from aqueous solution by biochar prepared from jackfruit peel: Isotherm model studies. *Vietnam Journal of Catalysis and Adsorption, 12*(1), 1–7. https://doi.org/10.51316/jca.2023.001

Wei, F., Jin, S., Yao, C., Wang, T., Zhu, S., Ma, Y., Qiao, H., Shan, L., Wang, R., Lian, X., Tong, X., Li, Y., Zhao, Q., & Song, W. (2023). Revealing the combined effect of active sites and intra-particle diffusion on adsorption mechanism of methylene blue on activated red-pulp pomelo peel biochar. *Molecules, 28*(11), Article 4426. https://doi.org/10.3390/molecules28114426